

SUPPORTING INFORMATION

PbS Quantum Dots as Additives in Methylammonium Halide Perovskite Solar Cells: the Effect of Quantum Dot Capping

Thi Tuyen Ngo,¹ Sofia Masi,¹ Perla F. Mendez,^{1,2} Miri Kazes,³ Dan Oron,³ and Iván Mora Seró^{1*}

¹ Institute of Advanced Materials (INAM), Jaume I University, 12006 Castellón, Spain

² Facultad de Ciencias Químico Biológicas, Universidad Autónoma de Sinaloa, Cd. Universitaria, Av. de las Américas y Josefa Ortiz S/N, 80000, Culiacán, Sinaloa, México

³ Department of Physics of Complex Systems, Weizmann Institute of Science, Rehovot 76100, Israel

*Corresponding Authors: sero@uji.es

1. Characterization of PbS_OA after the synthesis

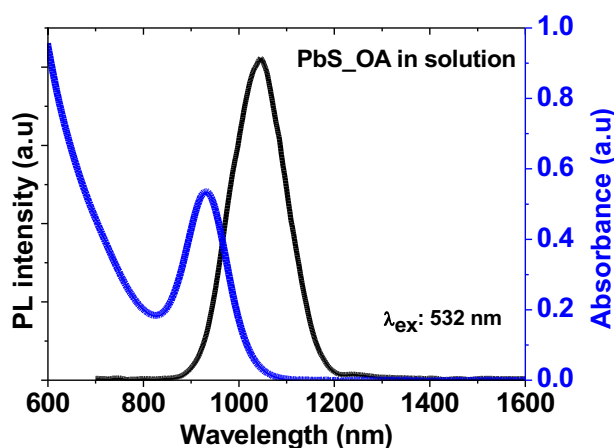


Fig S1. Photoluminescence (PL) and absorbance in solution of as-synthesized PbS QDs, with oleate ligands (OA), used in this work. For the PL measurement, an octane solution with a QD concentration of 0.196 mg/ml was used. A 532nm laser was used as the excitation source and a longpass filter 20CGA-590 was for photoluminescence measurements.

2. Ligand exchange process

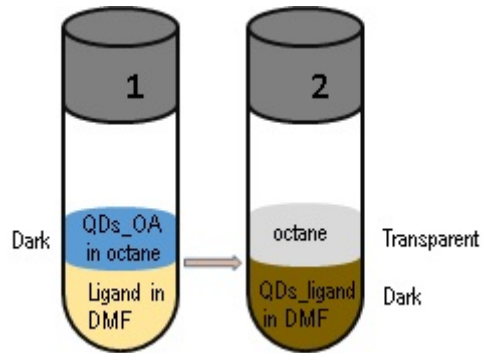


Fig S2. Phase transfer in the ligand exchange process of PbS QDs with 3 different ligands including 4-aminobenzoic acid (ABA), CsPI and MAPI. (1) Just mixing PbS_OA in octane with ligand in DMF. The top phase was dark which was PbS_OA dispersed in octane. The bottom phase was the ligand in DMF, which was yellow for MAPI and CsPI; colorless for ABA ligand. (2) After stirring/shaking the mixed solution, PbS QDs were transferred to the bottom phase, resulting the color change from dark to transparent of the top phase. Meanwhile the bottom phase became dark.

3. Characterization of PbS QDs after the ligand exchange

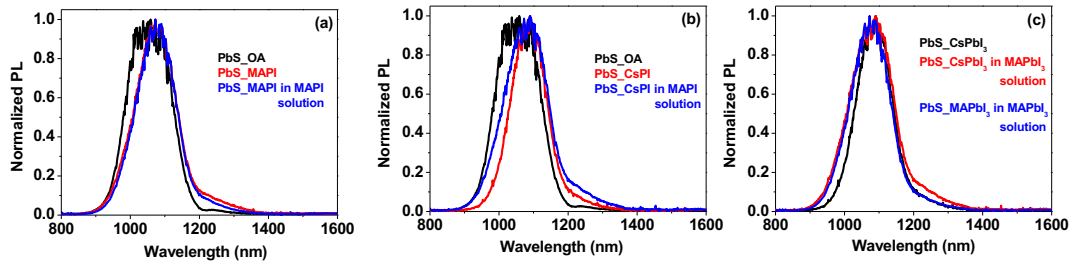


Fig S3. Photoluminescence (PL) in solution of PbS QDs before (as-synthesized, with OA capping ligand) and after the ligand exchange to MAPI (PbS_MAPI) and CsPI (PbS_CsPI); and after dispersing in HP perovskite precursor solution (PbI₂ and MAI). (a) PL spectra of the solutions correspond to MAPI and (b) CsPI capping ligands. (c) Comparison of PL of PbS_MAPI and PbS_CsPI in MAPI solution. PbS_OA QDs were dispersed in octane while PbS_MAPI and PbS_CsPI were dissolved in DMF. The solvent of PbS_MAPI or PbS_CsPI in MAPI solution was a mixture of DMF and DMSO with 10:0.95 volume ratio. The concentration of MAPI solution is 0.05 M. And the concentration of PbS QDs (with different capping ligands) was 1 mg/ml for all solutions. For the PL measurement, a laser of 532 nm was used as the excitation and a longpass filter 20CGA-590 was used in order to avoid the signal from the excitation source come to the CCD detector.

Fig. S3 presents the PL spectra of PbS before and after ligand exchange to MAPI and CsPI capping, and after dissolving in the solution containing MAPI precursors. In agreement with literature, after ligand exchange to both MAPI and CsPI, we observed a redshift in PL spectra.¹⁻³ As previously reported, ligand exchange to MAPI or CsPI results in the formation of a core/shell structure.²⁻³ This likely reduces the degree of quantum

confinement, leading the redshift in the PL spectra. Interestingly the PL spectrum of PbS_MAPI becomes narrower in comparison with as-synthesized PbS_OA QDs (see Fig. S3a), and the PL spectrum is narrowest for the case of exchange to CsPI (see Fig S3b). This may result from improved QD passivation.³ Moreover the PL spectra of PbS_MAPI and PbS_MAPI in a solution containing MAPI precursor are nearly identical, demonstrating the MAPI shell is not dissociated in the presence of MAPI precursors (see Fig S3a).¹ Notably, for the case of PbS_CsPI, after dissolving in the MAPI solution, the position of PL peak was maintained, yet the PL yield increased. For a better comparison, the PL spectrum of PbS_MAPI in MAPI solution was plotted together with PbS_CsPI and PbS_CsPI in MAPI solution (see Fig S3c). The PL of PbS_CsPI in MAPI solution was similar but not identical, suggesting that the CsPI shell interacts with MAPI precursors.

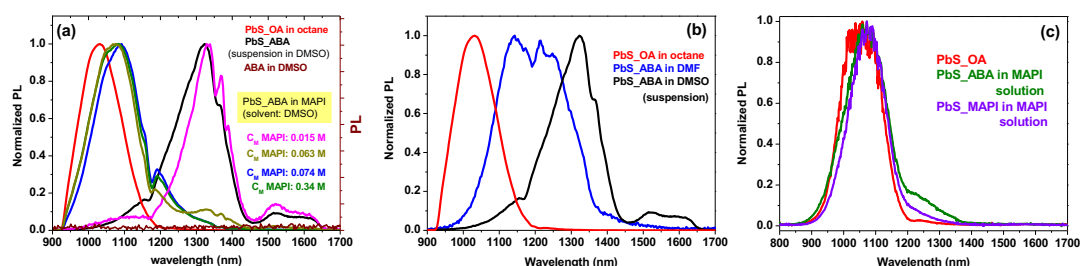


Fig S4. (a) Photoluminescence (PL) in solution of PbS QDs before (as-synthesized, with OA capping ligand) and after the ligand exchange to ABA capping (PbS_ABA) and after dispersing in a solution containing different concentration of HP precursors (PbI₂ and MAI). DMSO was the solvent for all solution in S4a except PbS_OA solution. The concentration of PbS in all solutions was ~ 0.46 mg/ml. (b) PL spectra of PbS_ABA in DMF and DMSO. (c) PL spectra of PbS_OA, PbS_ABA and PbS_MAPI in MAPI solution which was dissolved in a mixture of DMF and DMSO 10:0.95 v/v ratio. The concentration of PbS was 1 mg/ml for all solution in S4c. PbS_OA was dissolved in octane for all cases. PL spectra were measured using Fluorolog (a,b) and CCD systems (c). A 532 nm excitation wavelength and a longpass filter 20CGA-590 were used for both cases. The PL peak-shoulders wavelengths longer than 1100 nm probably due to the absorption of DMSO and DMF in the infrared.

Fig. S4a shows the PL spectra of PbS_OA, PbS_ABA in DMSO and PbS_ABA in DMSO in the presence of MAPI precursors with different concentrations. After ligand exchange to ABA, the solubility of PbS_ABA in DMSO is very limited and PbS_ABA QDs are unstable. They precipitate from DMSO after a short time, probably in one hour. The PL of PbS_ABA in DMSO (Fig S4a-b) was measured when PbS_ABA became precipitated (it is indicated as ‘suspension’). Because of the aggregation of PbS_ABA in DMSO, strong red-shifts in PL were observed, in comparison with as-synthesized PbS_OA QDs (Fig S4a). It is important to note that ABA does not fluoresce, at least under our measurement conditions (excitation and detected wavelength window). Interestingly, by adding the precursors of MAPI, the solubility of PbS_ABA in DMSO was improved. At a very low concentration of MAPI, 0.015 M, PbS_ABA QDs are partially dissolved illustrated by reducing in PL peak’s width at ~ 1300 nm and appearing the PL at ~ 1070 nm. And at 0.063 M of MAPI concentration, the solubility of PbS_ABA in DMSO was significantly enhanced. All the PL peaks at wavelengths longer than 1500 nm disappeared and a strong reduction in PL intensity (~ 90%) of PL peak at ~ 1300 nm was observed. At the same time, the intensity of PL peak at ~ 1070 nm strongly increased. When the

concentration of MAPI was increased to 0.074 M, aggregation of PbS_ABA was no longer observed, and the PL peak at ~ 1300 nm completely disappeared. Further increasing in MAPI concentration did not lead to any change in PL peak position. The improvement in PbS_ABA solubility in DMSO by the presence of MAPI precursors demonstrates a strong interaction of ABA and MAPI precursors.

As in the ligand exchange to ABA DMF was used instead of DMSO, we compared PbS_ABA dissolved in DMSO and DMF. We experimentally found that the solubility of and stability of PbS_ABA in DMF are better than that in DMSO. However PbS_ABA in DMF still produced a strong redshift in PL (see Fig S4b). It is important to note that from naked eyes the solution was completely lucent. Similar to the case of DMSO solvent, in DMF solvent and in the presence of MAPI precursors, PL of PbS_ABA became blueshifted, to very close to PbS_OA before the exchange (see Fig S4c). Interestingly in the presence of MAPI precursors, PbS_ABA produced a larger redshift in DMSO than in DMF (see Fig S4a and c), in a comparison with PbS_OA QDs, indicating the role of the solvent in determining the interaction of ABA with MAPI precursors. Notably, the PL position was compared at the same PbS QD concentrations, and the PL spectra of PbS_ABA and PbS_MAPI in the presence of MAPI precursors are different, as shown in Fig S4c, suggesting ABA still linked to PbS QDs.

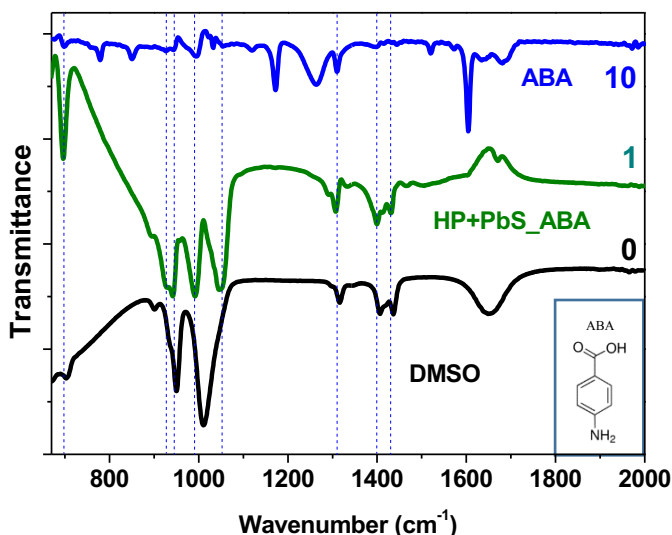


Fig S5. Fourier-transform infrared (FT-IR) measurement of DMSO, ABA solution in DMSO and HP+PbS_ABA in DMSO. Numbers correspond to amount of ABA in solutions. Number 1 is equivalent to 11.4 mg/ml. The concentration of PbS in HP+PbS_ABA solution is 8.3 mg/ml. Intensity of blue lines was triple. The samples were measured with DMSO as baseline. The insert presents the chemical structure of ABA.

Estimation of ABA amount. The ligand exchange from PbS_OA to PbS_ABA was described in the experimental section (section 2.2 in the main text). 2 ml of 0.025 M ABA in a mixture of DMF+absolute ethanol and 2 ml of 2.5 mg/ml PbS_OA in octane were introduced in the ligand exchange. After the ligand exchange, QDs were dried and dispersed in 0.6 ml of 1.33 M HP precursor solution (MAI and PbI₂), the olive line in Fig. S5b. Assuming there was no loss during the ligand exchange, the concentration of PbS QDs and ABA were:

$$C_{Pbs} = \frac{2 \text{ ml} \times 2.5 \text{ mg/ml}}{0.6 \text{ ml}} = 8.3 \left(\frac{\text{mg}}{\text{ml}} \right)$$

$$C_{ABA} = \frac{0.025 \frac{\text{mol}}{\text{l}} \times 137.14 \frac{\text{g}}{\text{mol}} \times 2 \text{ ml}}{0.6 \text{ ml}} = 11.4 \text{ mg/ml}$$

ABA in DMSO was prepared with concentration of 38 mg/ml and its FT-IR was triple, thus the concentration of ABA was considered as $38 \times 3 = 114 \text{ mg/ml}$ (corresponding to number 10, [blue line](#)).

The FT-IR measurement of ABA in DMSO shows a broad absorption with the appearance of many bands from 670 to 2000 cm^{-1} . The HP+PbS_ABA in DMSO exhibits the signals related to ABA. The band at 695 cm^{-1} , 990 cm^{-1} , 1050 cm^{-1} and 1307 cm^{-1} were observed probably due to the absorption of amine (N-H deformation vibration), aromatic carboxylic acid (O-H deformation vibration) and of carboxylic acid (C-O stretching and O-H deformation vibration) respectively.⁴ The intensity of those bands is more intense in a comparison with ABA in DMSO. It is important to note that the amount ABA in DMSO is much higher than that in HP+PbS_ABA solution. On the hand, two intense bands at 1174 cm^{-1} and 1263 cm^{-1} were observed for ABA solution but not for HP+PbS_ABA samples while bands at lower intensity listed above were obtained with even higher intensity. This suggests an interaction of ABA with MAPI precursors, also supported by the PL findings above. At 930 cm^{-1} and 1400 cm^{-1} HP+PbS_ABA in DMSO may have a signal related to ABA however the absorption of DMSO makes the analysis more complicated. The 1604 cm^{-1} band in ABA is probably due to the C=O stretching vibration of the carboxylic acid, and seems to shift to 1670 cm^{-1} in the hybrid film.

4. Characterization of HP+PbS QD films

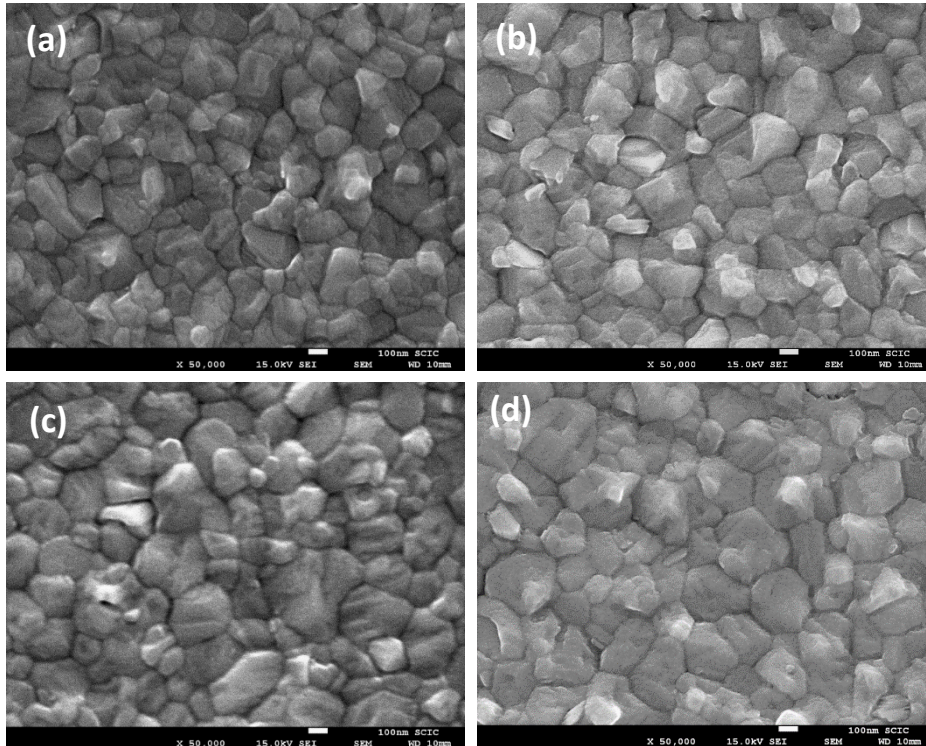


Fig S6. SEM of perovskite without (a) and with PbS QDs (50 $\mu\text{g/ml}$) in which PbS QDs had CsPI (b), MAPI (c) and 4-aminobenzoic acid (d) respectively. Bar scale in the figure was 100 nm.

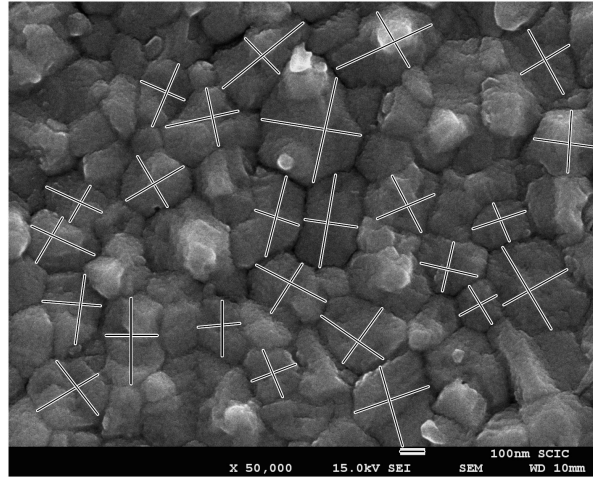


Fig S7. Estimation perovskite grain size from the top view SEM. The size of each grain is supposedly estimated by the average of two perpendicular lines crossing the grain with longest and shortest distance.

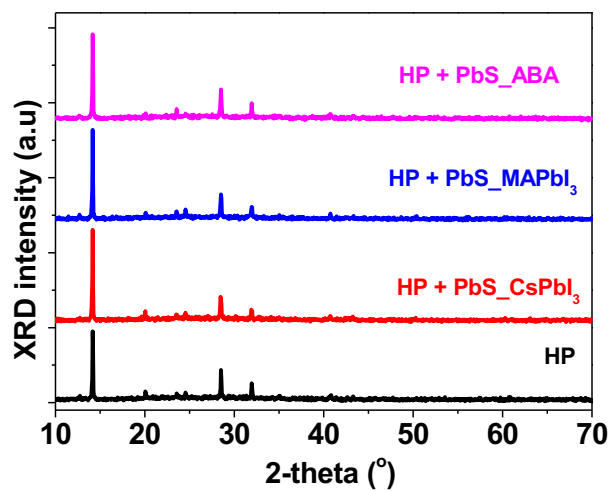


Fig S8. XRD of perovskite without (HP) and with PbS QDs (50 $\mu\text{g/ml}$) in which PbS QDs had CsPI, MAPI and 4-aminobenzoic acid respectively.

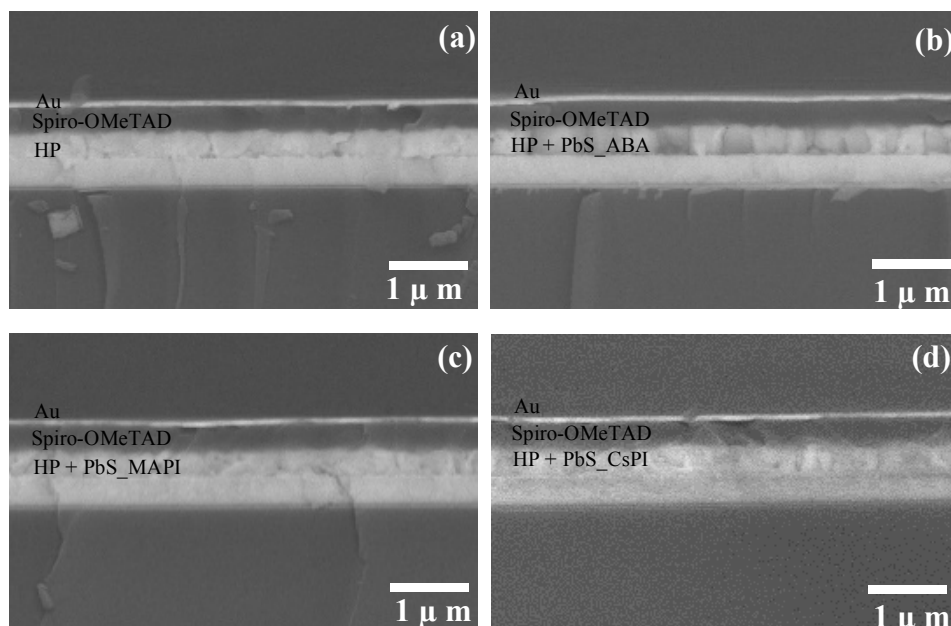


Fig S9. Cross section of FTO/SnO₂/absorber/spiro-OMeTAD/Au solar cells. In which absorber layer were perovskite (HP) without (a) and with PbS QDs 50 μg/ml (b-c) and 100 μg/ml (d). The ligand of PbS QDs were 4-aminobenzoic acid (ABA, b), MAPI (c) and CsPI (d).

5. Characterization of HP+PbS QD based devices

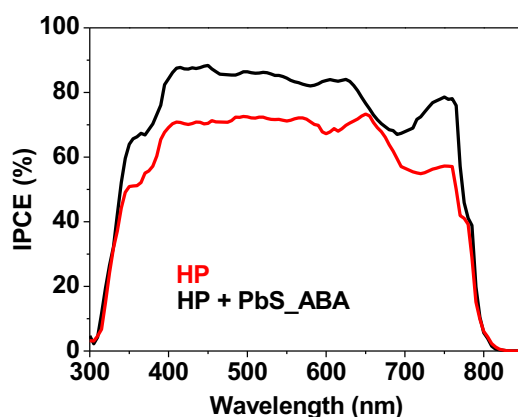


Fig S10. Incident photon to current efficiency (IPCE) of FTO/SnO₂/absorber/spiro-OMeTAD/Au solar cells, in which absorber layers were perovskite films without (HP) and with PbS QDs (50 μg/ml). The PbS QDs had 4-aminobenzoic acid (ABA) ligand.

References

1. Ngo, T. T.; Suarez, I.; Sanchez, R. S.; Martinez-Pastor, J. P.; Mora-Sero, I. Single step deposition of an interacting layer of a perovskite matrix with embedded quantum dots. *Nanoscale* **2016**, *8*, 14379-14383.
2. Yang, Z.; Janmohamed, A.; Lan, X.; García de Arquer, F. P.; Voznyy, O.; Yassitepe, E.; Kim, G.-H.; Ning, Z.; Gong, X.; Comin, R.; Sargent, E. H. Colloidal Quantum Dot Photovoltaics Enhanced by Perovskite Shelling. *Nano Letters* **2015**, *15* (11), 7539-7543.

3. Zhang, X.; Zhang, J.; Phuyal, D.; Du, J.; Tian, L.; Öberg, V. A.; Johansson, M. B.; Cappel, U. B.; Karis, O.; Liu, J.; Rensmo, H.; Boschloo, G.; Johansson, E. M. J. Inorganic CsPbI₃ Perovskite Coating on PbS Quantum Dot for Highly Efficient and Stable Infrared Light Converting Solar Cells. *Advanced Energy Materials* **2018**, *8* (6), 1702049.
4. Socrates, G. *Infrared and Raman characteristic group frequencies: tables and charts*. John Wiley & Sons: 2004.